Excited-State Proton Transfer of Firefly Dehydroluciferin

ARTICLE *in* THE JOURNAL OF PHYSICAL CHEMISTRY A · OCTOBER 2012

Impact Factor: 2.69 · DOI: 10.1021/jp308818r · Source: PubMed

8 AUTHORS, INCLUDING:

Yuval Erez
Weizmann Institute of Science
38 PUBLICATIONS **468** CITATIONS
SEE PROFILE

Luís Pinto da Silva
University of Porto
55 PUBLICATIONS **448** CITATIONS
SEE PROFILE

Joaquim C G Esteves da Silva
University of Porto
302 PUBLICATIONS **2,943** CITATIONS
SEE PROFILE

THE JOURNAL OF PHYSICAL CHEMISTRY A

Article

pubs.acs.org/JPCA

Excited-State Proton Transfer of Firefly Dehydroluciferin

Itay Presiado,[†] Yuval Erez,[†] Ron Simkovitch,[†] Shay Shomer,[†] Rinat Gepshtein,[†] Luís Pinto da Silva,[‡] Joaquim C.G. Esteves da Silva,[‡] and Dan Huppert*,[†]

[†]Raymond and Beverly Sackler Faculty of Exact Sciences, School of Chemistry, Tel Aviv University, Tel Aviv 69978, Israel

[‡]Centro de Investigação em Química, Departamento de Quimica, Faculdade de Ciencias da Universidade do Porto, R. Campo Alegre 687 4169-007 Porto, Portugal

Supporting Information

ABSTRACT: Steady-state and time-resolved emission techniques were used to study the protolytic processes in the excited state of dehydroluciferin, a nonbioluminescent product of the firefly enzyme luciferase. We found that the ESPT rate coefficient is only 1.1×10^{10} s^{-1}, whereas those of D-luciferin and oxyluciferin are 3.7×10^{10} and 2.1×10^{10} s^{-1}, respectively. We measured the ESPT rate in water−methanol mixtures, and we found that the rate decreases nonlinearly as the methanol content in the mixture increases. The deprotonated form of dehydroluciferin has a bimodal decay with short- and long-time decay components, as was previously found for both D-luciferin and oxyluciferin. In weakly acidic aqueous solutions, the deprotonated form's emission is efficiently quenched. We attribute this observation to the ground-state protonation of the thiazole nitrogen, whose pK_a value is ∼3.

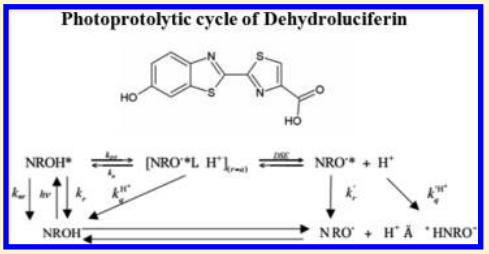

INTRODUCTION

Bioluminescence is an enzyme-catalyzed reaction, in which an excited-state product is formed and visible light is emitted.[1−3] This enzyme is always termed luciferase regardless of the organism in which it is found.[1−3] The most studied bioluminescence system is that of the fireflies due to their highly efficient luminescence.[1−4] Light is emitted by firefly oxyluciferin, which is formed due to a luciferase-catalyzed two-step reaction .[5,6]

Oxyluciferin (Scheme 1) is usually thought to exist in one of six chemical forms by means of a quadruple chemical equilibrium. However, several groups have demonstrated that oxyluciferin is formed in the anionic keto form during the bioluminescence reaction but exists in an enol form in solution.[7−10]

Scheme 1. Keto−Enol Tautomerism Equilibrium of Oxyluciferin

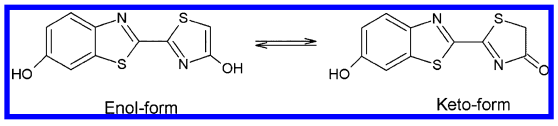

Despite the difficulties associated with the experimental study of oxyluciferin, it was found that its absorption spectrum has a band at ∼440 nm for basic pH and one at ∼370 at acidic-neutral pH.[10,11] The emission spectra were found to be characterized by a peak at ∼550 nm at acidic-neutral pH and a peak at 540 nm at basic pH.[11] We have also found that oxyluciferin is a photoacid with an ESPT rate of 2.2×10^{10} s^{-1}. It also undergoes fluorescence quenching stemming either from geminate recombination with the proton or from excess protons in acidic media.[11]

D-Luciferin (Scheme 2) is one of the most useful analogues of the keto form of oxyluciferin, aside from being one of the substrates of the bioluminescence reaction. The absorption spectrum of this molecule is characterized by a maximum at ∼330 nm in acidic solution, and it is red-shifted at basic pH (∼390 nm).[11−16] The emission spectrum of D-luciferin has a maximum at ∼530 nm over the studied pH range of 3−10.[11−16] However, a decrease in the polarity of the solvent uncovers an emission band with a maximum at ∼450 nm.[11−16] The red shift with increasing pH and polarity of the solvent is attributed to the deprotonation of the benzothiazole hydroxyl group. In strongly acidic solutions, an emission band at ∼590 nm is found, which corresponds to the protonation of one of the nitrogen heteroatoms. We have also found that D-luciferin is a photoacid with an ESPT rate of 3.7×10^{10} s^{-1}. It also undergoes fluorescence quenching stemming either from geminate recombination with the proton or from excess protons is acidic media.[11−16]

Scheme 2. Chemical Structures of D-Luciferin and L

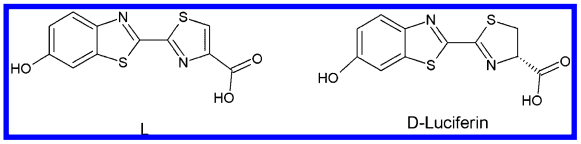

Received: September 5, 2012
Revised: October 10, 2012
Published: October 11, 2012

Firefly luciferase can also catalyze the formation of other nonbioluminescent products in dark lateral side reactions. In the presence of PP_i and dehydroluciferyladenylate (which is also produced in dark lateral reaction), luciferase can catalyze the formation of dehydroluciferin (L) (Scheme 2).[17−20] This molecule is an analogue of both oxyluciferin and D-luciferin. More importantly, while D-luciferin is more of an analogue of the keto form of oxyluciferin (due to the absence of a C═C double bond in the thiazole moiety), L is more of an analogue of the enol form of oxyluciferin (due to the presence of a C═C double bond in the thiazole moiety) (Scheme 2). This can be seen by the fact that at neutral-acidic pH, L has the same emission wavelength as oxyluciferin in aqueous solution (~550 nm).[21] Therefore, studying the spectroscopic properties and photoprotolytic cycle of this molecule can give us more insight into the spectroscopic properties of oxyluciferin in solution by bypassing the difficulties associated with experimenting with oxyluciferin itself. Moreover, the fact that luciferase can produce a fluorescent compound in a dark lateral reaction means that its bioluminescence reaction can affect the analysis of results obtained in spectroscopic studies of the luciferase−luciferin complex. Thus, there is the need for a more complete characterization of the photophysical properties and photoprotolytic cycle of L.

EXPERIMENTAL SECTION

(4*S*)-2-(6-Hydroxybenzothiazole-2-yl)-4,5-dihydrothiazole-4-carboxylic acid (D-luciferin) 99.5% was purchased from Iris Biotech (Germany). HCl (1 N) was purchased from Aldrich. Chemically synthesized oxyluciferin was obtained from 2-cyano-6-hydroxybenzothiazole and ethyl thioglycolate.[22] The parent compound 2-cyano-6-hydroxybenzothiazole was obtained from 2-cyano-6-methoxybenzothiazole (Aldrich, Steinheim, Germany).[8,20] L was chemically synthesized and purified as described previously.[20,22,23] For transient measurements, the sample concentrations were between 2×10^{-4} and 2×10^{-5} M. Deionized water had a resistance of >10 MΩ. Methanol of analytical grade was purchased from Fluka. All chemicals were used without further purification.

The fluorescence up-conversion technique was employed in this study to measure the time-resolved emission of L at room temperature. The laser used for the fluorescence up-conversion was a cavity-dumped Ti:Sapphire femtosecond laser, Mira, Coherent, which provides short, 150 fs, pulses at around 800 nm. The cavity dumper operated with a relatively low repetition rate of 800 kHz. The up-conversion system (FOG-100, CDP, Russia) operated at 800 kHz. The samples were excited by pulses of ~8 mW on average at the SHG frequency. The time response of the up-conversion system is evaluated by measuring the relatively strong Raman−Stokes line of water shifted by 3600 cm^{-1}. It was found that the fwhm of the signal is 300 fs. Samples were placed in a rotating optical cell to avoid degradation.

We used the time-correlated single-photon counting (TCSPC) technique to measure the time-resolved emission of L. The second harmonics (SHG) of the same laser described above, operating over the spectral range of 380−420 nm, was used to excite the photoacid samples. The TCSPC detection system is based on a Hamamatsu 3809U, photomultiplier, and Edinburgh Instruments TCC 900 computer module for TCSPC. The overall instrumental response was about 40 ps (fwhm). The excitation pulse energy was reduced to about 10 pJ by neutral density filters.

RESULTS

Figure 1 shows the excitation and fluorescence spectra of L in both H_2O and D_2O at slightly acidic samples (pH ≃ 6). The excitation spectrum was acquired at λ_{em} = 600 nm. For the emission spectrum, the sample was excited at 360 nm, and it consisted of a weak band with a peak at ~446 nm and a stronger band with a peak at ~550 nm. We attribute the two emission bands to the protonated NROH* and deprotonated NRO^-* forms of L, which, like D-luciferin and oxyluciferin (shown in Scheme 2), is a photoacid, and therefore, it undergoes a photoprotolytic process (shown in Scheme 3)

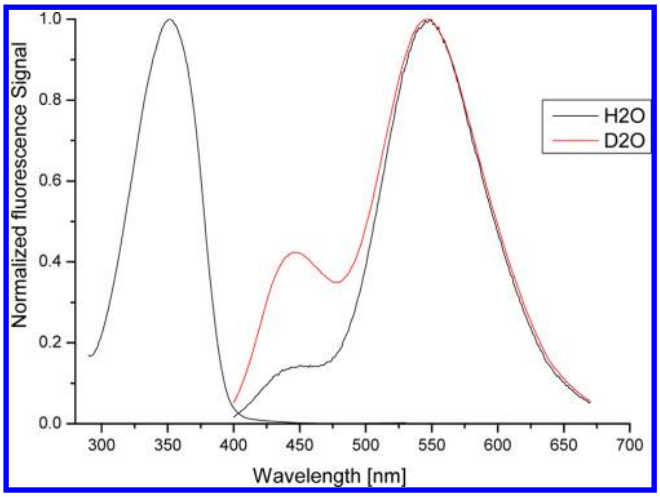

Figure 1. Excitation and fluorescence spectra of L in both H_2O and D_2O at slightly acidic samples (pH ≃ 6). The excitation spectrum was acquired at λ_{em} = 600 nm. For the emission spectrum, the sample was excited at 360 nm, and it consists of a weak band with a peak at ~446 nm and a stronger band with a peak at ~550 nm.

Scheme 3. Photoprotolytic Cycle of D-Luciferin, Oxyluciferin, and L

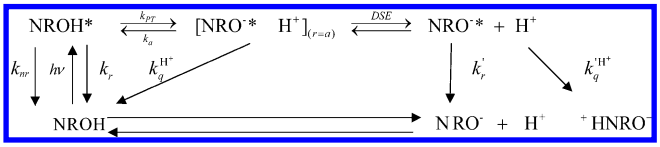

when the NROH form is electronically excited from its ground state. The NROH* form is a stronger acid than NROH. It transfers a proton to the solvent and becomes the deprotonated NRO^-* form within the excited-state lifetime. This ESPT process leads to the dual-band emission spectrum shown in Figure 1. The ESPT rate coefficient, k_{PT}, depends on the isotopic species that is transferred (H_3O^+/D_3O^+). The kinetic isotope effect (KIE) on k_{PT} for photoacids is usually around 3.[24] For both D-luciferin and oxyluciferin, we previously found a KIE value of ~2.5.[11] The steady-state emission is affected by the isotopic composition of the sample. The ratio between the intensities of the protonated and deprotonated forms of the bands in D_2O is higher than that in H_2O, as can be seen in Figure 1. We discuss the KIE in more detail later on.

Time-Resolved Emission. Figure 2 shows the fluorescence up-conversion time-resolved emission signal of L in aqueous solution. At $\lambda \leq 450$ nm, the signal consists of two components. The short-time component of about 1 ps and a relative amplitude of 0.2 at 440 nm is attributed to solvation dynamics,

dx.doi.org/10.1021/jp308818r | J. Phys. Chem. A 2012, 116, 10770−10779

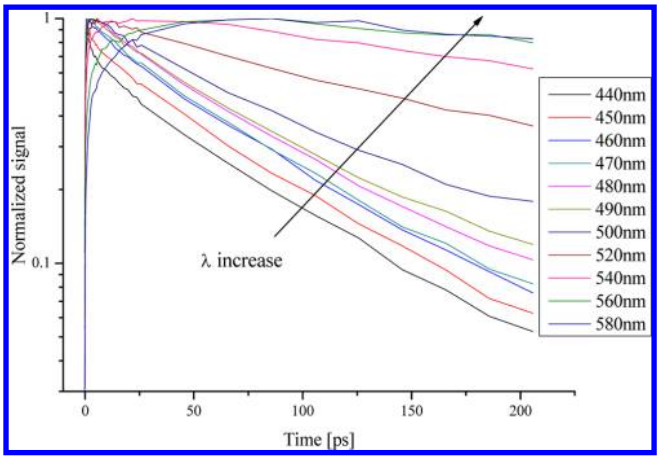

Figure 2. Fluorescence up-conversion time-resolved emission signal of L in aqueous solution.

which shifts the NROH* emission band to the red. The major component's decay is nonexponential with an average decay time of ~80 ps. At 460–490 nm, the short-time component disappears; therefore, the decay curve virtually consists of just the long-time component. A good fit to the nonexponential fluorescence up-conversion signals of the NROH* was obtained using a stretched exponent, $\exp[(-t/\tau)^{\alpha}]$, where $\alpha = 0.8$ and $\tau = 60$ ps. We attribute this component to the ESPT process of L. At $\lambda \geq 540$ nm, the signal consists of a distinctive rise component, followed by a long decay time. We attribute this emission signals to the formation of the excited deprotonated NRO^{-}* form by the photoprotolytic reaction described in Scheme 3.

Figures 3 and S1 in the SI show the time-resolved emission of L in aqueous solution detected at several wavelengths in the

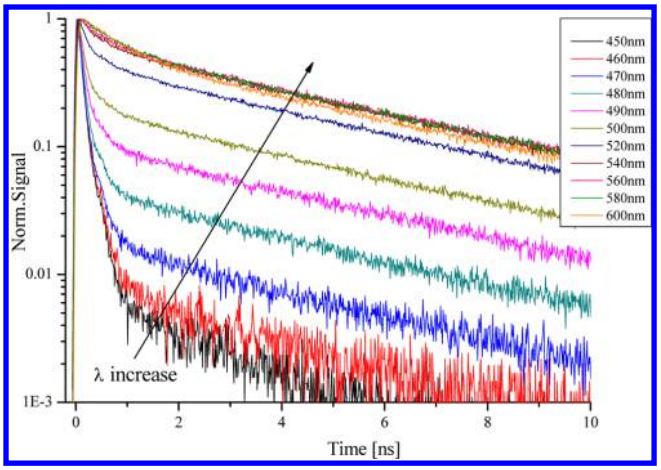

Figure 3. Time-resolved emission of L in aqueous solution detected at several wavelengths in the range of 450–600 nm on a semilogarithmic scale.

range of 450–600 nm on semilogarithmic and linear scales. The sample was excited by short ~150 fs laser pulses at ~387 nm. The excitation and detection of the time-resolved signal were carried out by the TCSPC technique, which has a wide dynamic range yet a limited time resolution of 20 ps because the instrument's response function (IRF) has a full width half-maximum (fwhm) of 40 ps. The signals in the range of 450–480 nm consist of a major decay component with an amplitude of 0.99 and a decay time constant of 88 ps and a longer minor decay component with a very small amplitude. The fast decay component arises from ESPT to the solvent. For D-luciferin and oxyluciferin, this time constant was significantly shorter, that is, 27 and 47 ps, respectively. We therefore conclude that the ESPT rate coefficients of D-luciferin, oxyluciferin, and L are 3.7×10^{10}, 2.1×10^{10}, and 1.1×10^{10} s^{-1}, respectively.

At $\lambda \geq 540$ nm, much of the signal arises from the emission of the deprotonated form, that is, the product of the photoprotolytic reaction. The TCSPC signal of L at these wavelengths could be divided into three time domains. The short-time domain from $t = 0$ until the signal's maximum is 100 ps in length. The rise of the signal is attributed to the formation of the NRO^{-}* form by the photoprotolytic reaction and the ~40 ps fwhm of the IRF. The second time domain stretches from the maximum to about $t = 1$ ns. It has a decay time of ~600 ps, and the intensity of the signal within this domain is reduced by about 35%. We attribute this component to ESPT from the hydroxyl group on the benzothiazole to a nitrogen on the thiazole ring via a water bridge made of one or two water molecules. Nitrogen in a heterocyclic ring is known to be a stronger base in the excited state.[25] It is also known that excited-state protonation of this nitrogen leads to fluorescence quenching. The time-resolved emission signals of both D-luciferin and oxyluciferin have similar fluorescence quenching intermediate time components. The long-time component of the time-resolved fluorescence decays exponentially with a time constant of 5.2 ns. This component is attributed to the radiative decay process of L. Similar radiative lifetimes exist for the fluorescence signals of both D-luciferin and oxyluciferin.[11]

Kinetic Isotope Effect. Figures 4 and S2 in the SI show on semilogarithmic and linear scales the time-resolved emission of L in both H_2O and D_2O. At $\lambda \leq 480$ nm, the TCSPC fluorescence decay signal provides the proton/deuteron transfer rate. At long wavelengths, the rise of the signal is indicative of the buildup of the deprotonated form's population. The NROH* and NRO^{-}* emission bands overlap at $\lambda > 520$ nm, and thus, TCSPC signals in that spectral region are the result of superposition of both emission bands. The time-resolved emission signal at frequency ν and time t is given by

$$I_F(\nu, t) = f_{NROH^*} \cdot g_{NROH^*}(\nu) \cdot F_{NROH^*}(t) + f_{NRO^{-}*} \cdot g_{NRO^{-}*}(\nu) \cdot F_{NRO^{-}*}(t) \quad (1)$$

where f_{NROH^*} and $f_{NRO^{-}*}$ are the oscillator strengths of the NROH* and NRO^{-}* emission bands, respectively, and $g_{NROH^*}(\nu)$ and $g_{NRO^{-}*}(\nu)$ are the line shape functions of the two bands. For simplicity, we assume that the line shapes of the two emission bands are constant in time. The time dependence of the NROH* band given in the term $F_{NROH^*}(t)$ is complex because the geminate recombination with the proton repopulates the NROH* state, and it causes the fluorescence decay curve to become nonexponential. The fluorescence decay of the NRO^{-}* of L, $F_{NRO^{-}*}(t)$, and other luciferins is complex because of the proton-assisted nonradiative process, that is, protonation of the heterocyclic nitrogen. The KIE on the time-resolved fluorescence of L and the two other luciferins at $\lambda \leq 480$ nm is relatively strong. We found a KIE value of 2.4 for L and 2.5 for D-luciferin and oxyluciferin. The structure of L (see Scheme 2) is simpler than that of oxyluciferin, which can exist in six different tautomers, where proton transfer can occur only from the two tautomers shown in Scheme 1. The reproducibility of the KIE values indicates that ESPT occurs

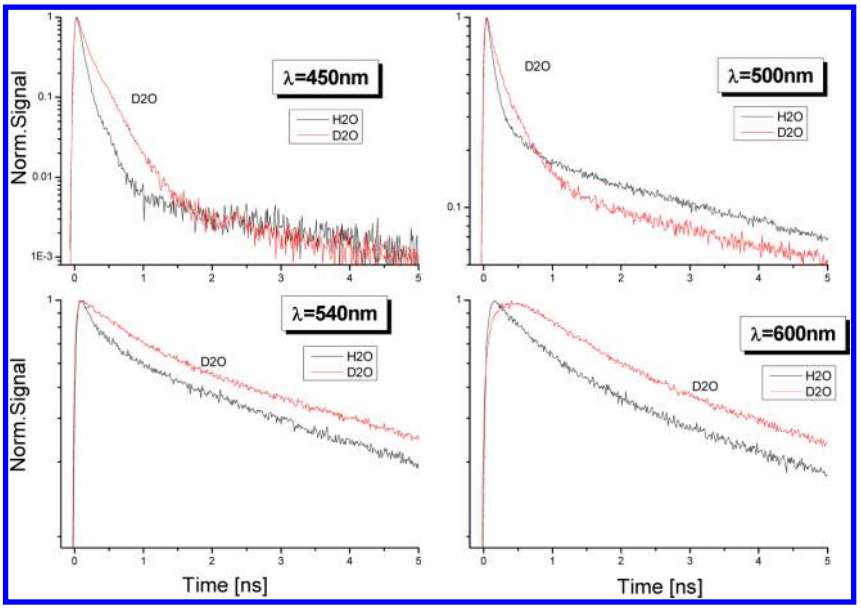

Figure 4. Time-resolved emission of L in both H_2O and D_2O on a semilogarithmic scale. At $\lambda \leq 480$ nm, the TCSPC fluorescence decay signal provides the proton/deuteron transfer rate.

from the hydroxyl group in L, where the hydroxyl is the only functional group capable of ESPT, but also in the other two luciferins. In the range of 490−530 nm, the relative amplitudes of the two bands rapidly change, from a large amplitude for the NROH* band and a small amplitude for the NRO^-* band at 490 nm to about equal amplitudes at ~520 nm. At $\lambda \geq 540$ nm, the relative amplitude of the NRO^-* signal is larger than that of the NROH*. In D_2O at 600 nm, the time-resolved signal clearly has a rise component stemming from the formation of the NRO^-* form via the photoprotolytic reaction. The formation time in D_2O is 2.5 times longer than that in H_2O. The biexponential fitting parameters to the TCSPC signals of L at various wavelengths in both H_2O and D_2O are given in Tables 1 and 2.

Table 1. Parameters of Time-Resolved Biexponential Analysis of Dehydroluciferin in H_2O

λ [nm]	τ_1 [ps]	b_1	τ_2 [ns]	b_2	χ^2
450	80	0.99	2.3	0.01	0.813
460	80	0.98	2.9	0.02	0.769
470	80	0.97	4.2	0.03	1.103
480	90	0.95	4.7	0.05	1.082
490	100	0.90	4.8	0.10	1.079
500	126	0.80	4.9	0.20	1.636
520	300	0.54	5.0	0.46	1.334
540	535	0.40	5.1	0.60	0.949
560	660	0.37	5.1	0.64	0.872
580	780	0.41	5.1	0.59	0.953
600	890	0.58	5.2	0.42	0.896

Comparing the Time-Resolved Emissions of the Three Luciferin Chromophores. In the past, we studied both D-luciferin and oxyluciferin with the same spectroscopic techniques.[11−16] In the current article, we wish to compare the steady-state and time-resolved spectra of the three compounds.

Figure 5a shows the time-resolved emission of the protonated forms of the three luciferins measured by the fluorescence up-conversion technique. As can be clearly seen, the decay time of NROH* of L is the longest. The decay time of D-luciferin is much shorter than L. As seen in Scheme 2, the two luciferins have similar structures. The difference lies in the thiazole ring, where the single bond of D-luciferin becomes a double C═C bond. This change accounts for the difference in the ESPT rates of a factor of 3.

Table 2. Time-Resolved Biexponential Analysis of Dehydroluciferin in D_2O

λ [nm]	τ_1 [ps]	b_1	τ_2 [ns]	b_2	χ^2
450	220	0.76	2.3	0.24	0.986
460	250	0.74	3.5	0.26	1.207
470	270	0.74	4.8	0.26	1.025
480	272	0.70	5.1	0.30	0.865
490	290	0.47	5.6	0.53	1.109
500	320	0.38	5.7	0.62	0.921
520	480	0.24	5.8	0.76	0.893
540	950	0.15	5.9	0.85	0.895
560	1300	0.27	6.0	0.73	0.801
580	1300	0.28	6.1	0.72	0.761

Figures 5b and S3 in the SI show the TCSPC signals of the three luciferin molecules on linear and semilogarithmic scales. At 450 nm, the time-resolved emission signal is greatly affected by the ESPT rate, whose time constants are 27, 47, and 88 ps for D-luciferin, oxyluciferin, and L, respectively. 2-Naphthol and 2-naphtholsulfonate derivatives are well-studied photoacids.[26] The ESPT rate from these molecules depends on the number of sulfonate groups and their positions in the molecule. For example, the ESPT time constants are 10 ns, 1 ns, and 40 ps for 2-naphthol, 2-naphthol-6-sulfonate, and 2-naphthol-6,8,-disulfonate, respectively. The differences in the ESPT rates can be explained by the Hamet relation and also by the Förster cycle. In the case of the three luciferins, the ESPT rates differ by much smaller values, and the reasons for them are yet unknown.

ESPT of L in Water−Methanol Mixtures. The photoacidity and the ESPT rate of photoacids with $pK_a^* \geq 0$ decrease

dx.doi.org/10.1021/jp308818r | J. Phys. Chem. A 2012, 116, 10770−10779

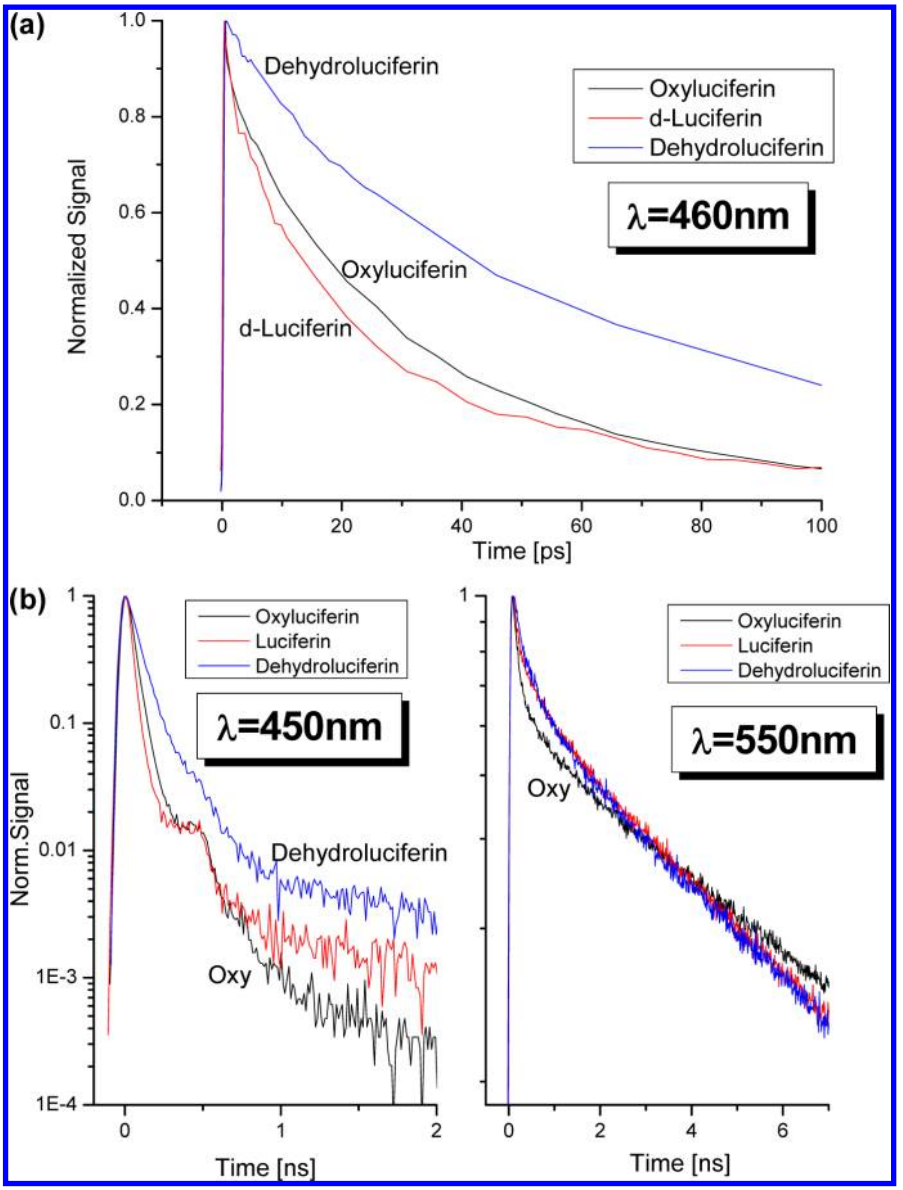

Figure 5. (a) Time-resolved emission of the protonated forms of the three luciferins measured by the fluorescence up-conversion technique. (b) TCSPC signals of the three luciferin molecules on a semilogarithmic scale.

by more than 2 orders of magnitude in methanol. The ESPT rates of L and 2-naphthol-6,8-disulfonate in water are 1.1×10^{10} and 2.0×10^{10} s^{-1}, respectively. On the basis of the free-energy relation between the ESPT rate and the pK_a*, we estimate the value of the latter to be 0.7 for L and 0.4 for 2-naphthol-6,8-disulfonate. 8-Hydroxypyrene-1,3,6-trisulfonate (HPTS) is a well-studied reversible photoacid with a pK_a* of ∼1.3 and an ESPT rate coefficient of 10^{10} s^{-1} in water.[24] It cannot transfer a proton within the time frame of the excited state in neat methanol.

Figure 6 shows the steady-state emission spectra of L in several water−methanol mixtures. In pure methanol, the emission spectrum consists of only the NROH* emission band because the ESPT rate is slower than the radiative rate, which means that the efficiency of the ESPT process is very low. In a 10% aqueous solution of methanol (the lowest concentration of methanol in which L is soluble to an appreciable degree), the emission spectrum is composed of two emission bands. The weak band belongs to the NROH*

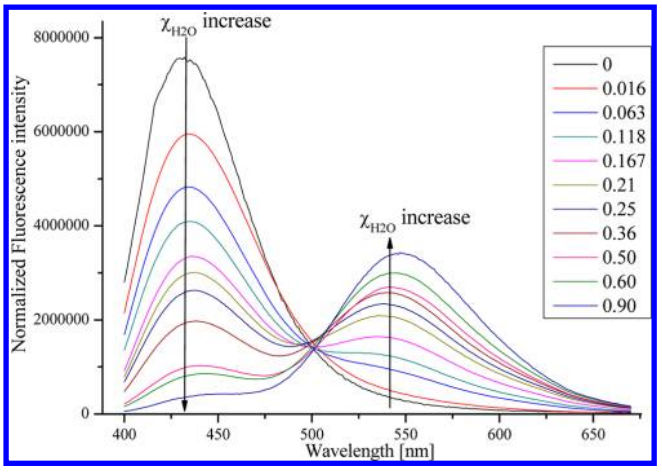

Figure 6. Steady-state emission spectra of L in several water−methanol mixtures.

dx.doi.org/10.1021/jp308818r | J. Phys. Chem. A 2012, 116, 10770−10779

form, whereas the strong band is that of the NRO^-* band. The less methanol there is in the mixture, the larger the intensity ratio becomes because the ESPT rate increases. This fluorescence intensity ratio is approximately given by the following expression:

$$I_{RO^-*}/I_{ROH*} \simeq \frac{k_{PT}}{k_F}\cdot\frac{k'_F}{k_F} \quad (2)$$

where k_F and k'_F are the reciprocals of the emission lifetimes of the NROH* and NRO^-* forms. It should be noted that k_F can be estimated from the emission of the NROH* form in the absence of an ESPT process by measuring the fluorescence decay in neat alcohols, where ESPT cannot occur. For the luciferins, the NRO^-* emission decay is not simply exponential with a rate coefficient k'_F because a proton-assisted quenching process take place, which further complicates the measurement of k_{PT} from the steady-state emission spectrum.

Figures 7 and S4 in the SI show on semilogarithmic and linear scales the time-resolved emission of L measured at 450

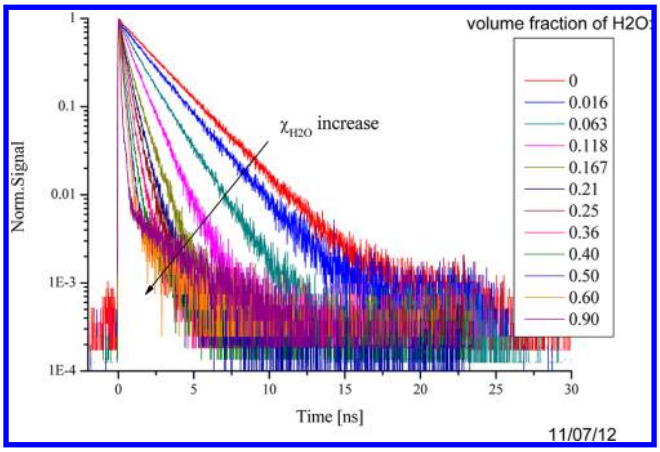

Figure 7. Time-resolved emission of L measured at 450 nm in water–methanol mixtures on a semilogarithmic scale. As seen in the figure, the fluorescence decay rate of the NROH* form increases the higher the water content in the mixture.

nm in water–methanol mixtures. As seen in the figures, the fluorescence decay rate of the NROH* form increases the higher the water content in the mixture. The decay of the signals shown in Figure 7 on a semilogarithmic scale is nearly exponential for more than 2 orders of magnitude for all of the mixtures that we measured. This implies that the geminate recombination taking place after proton transfer is irreversible. This is also verified in the time-resolved emission monitored at 550 nm, near the peak of the NRO^-* band. The decay of the NRO^-* signals in these mixtures is nonexponential, and their shape on a semilogarithmic scale is concave. This is due to the irreversible recombination process with the proton, which is characteristic for all luciferins that we studied, including L. Table 3 provides the decay times of the NROH* band in various water–methanol mixtures.

Acid Effect. For 1-naphthol and 1-naphtholsulfonate derivatives, which are simple irreversible photoacids carrying a hydroxyl group, addition of a strong mineral acid, such as HCl, leads to fluorescence quenching of the RO^-* emission by the reaction $RO^-* + H^+ \rightarrow ROH*$.[27] This, we found, is also true for the luciferins.

Table 3. Average Lifetimes for Dehydroluciferin in MeOH/H_2O Mixtures; λ = 450 nm

volume fraction of H_2O	τ_{ave} [ns]
0	2.334
0.016	1.90
0.063	1.349
0.118	0.929
0.167	0.611
0.21	0.506
0.25	0.426
0.36	0.353
0.4	0.274
0.5	0.217
0.6	0.178
0.9	0.11

We conducted steady-state and time-resolved studies of L in the presence of HCl in the solution in concentrations ranging from 10^{-4} to 10^{-1} M. Figure 8 shows the steady-state emission

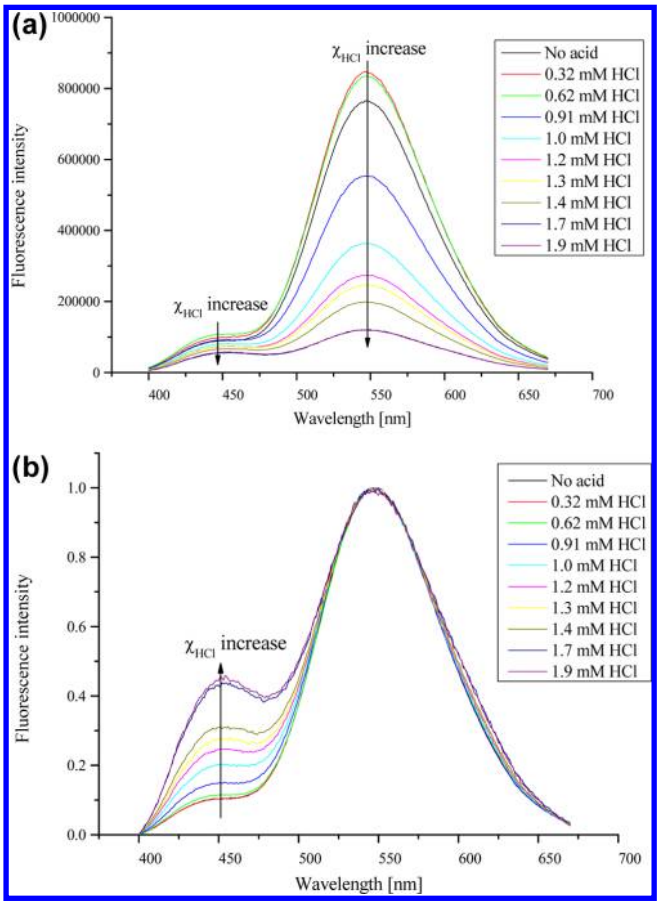

Figure 8. Steady-state emission spectra of L in acidic aqueous solutions with acid concentrations in the range of 10^{-4}–3×10^{-3} M; (a) non-normalized; (b) normalized.

spectra of L in 10% acidic aqueous solutions of methanol with acid concentrations in the range of 10^{-4} to 3×10^{-3} M. The intensity of both the NROH* and NRO^-* bands is reduced in the presence of HCl, although its effect is much stronger on the NRO^-* band than that on the NROH* band.

Figure 9a shows the time-resolved emission of L measured at 550 nm near the peak of the NRO^-* emission band. The

dx.doi.org/10.1021/jp308818r | J. Phys. Chem. A 2012, 116, 10770–10779

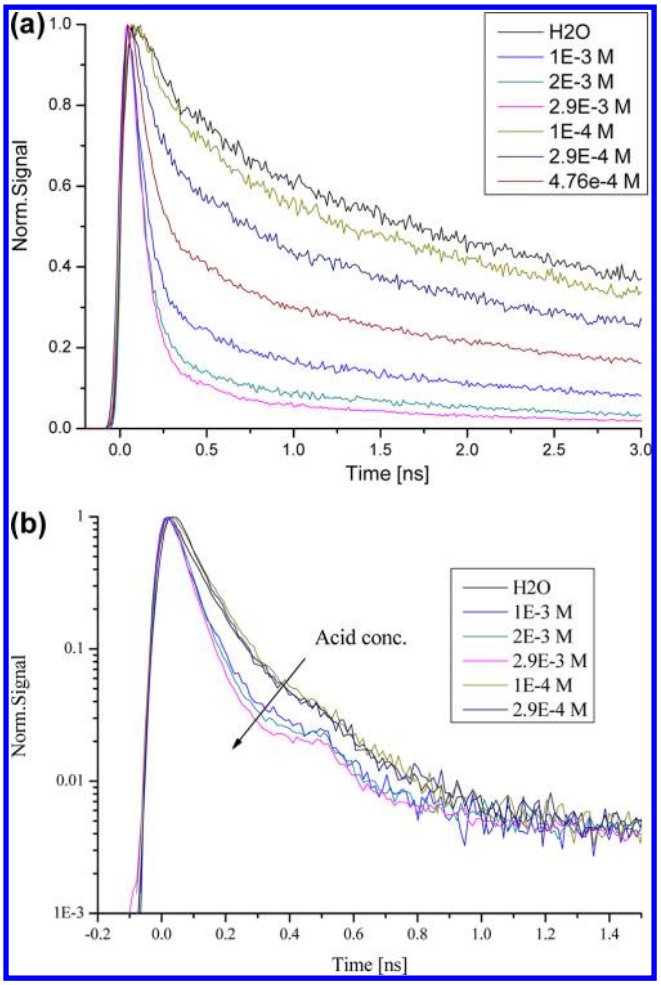

Figure 9. Time-resolved emission of L in various aqueous solutions of HCl measured at (a) 550 nm near the peak of the NRO^-* emission band and (b) 450 nm near the peak of the NROH* band.

fluorescence decay of the NRO^-* signal is bimodal with short- and long-time decay components. The amplitude of the short-time decay component increases with the acid concentration. The lifetime of this component decreases as the acid concentration increases. The lifetime of the long-time decay component is nearly invariant under change of the acid concentration in the range of 10^{-4}–10^{-3} M. At higher concentrations, the long decay time decreases as the acid concentration increases.

Figure 9b shows the time-resolved emission of L in the presence of HCl at the same concentrations as those shown in Figure 9a and measured at 450 nm, near the peak of the NROH* emission band. The decay of the NROH* signals is unaffected by the presence of HCl in the range of 10^{-5}–10^{-4} M. At higher concentrations, the fluorescence decay is shorter, that is, in neutral pH in water, the NROH* decay time is 90 ps, whereas in 1–10 mM, it is less than 50 ps. Table 4 provides the biexponential fitting parameters of both the NROH* and NRO^-* emission bands measured at 450 and 550 nm, respectively.

Main Findings. The main findings are as follows:

1. L is an irreversible photoacid with poor solubility in water.
2. The ESPT rate coefficient is 1.1×10^{10} s^{-1}, which is a value twice as small as that of oxyluciferin and three times smaller than that of D-luciferin.

Table 4. Biexponential Fits for Dehydroluciferin: Acid Effect

	For λ = 450 nm			
C_{HCl}	a_1	τ_1 [ps]	a_2	τ_2 [ns]
no acid	0.996	80	0.004	3.0
1×10^{-4} M	0.95	85	0.05	2.9
2.9×10^{-4} M	0.95	75	0.05	2.9
1 mM	0.996	50	0.004	2.3
2 mM	0.996	<50	0.004	2.3
2.9 mM	0.996	<50	0.004	2.3
	For λ = 550 nm			
C_{HCl}	a_1	τ_1 [ns]	a_2	τ_2 [ns]
no acid	0.33	0.35	0.67	0.42
1×10^{-4} M	0.4	0.28	0.6	4.2
2.9×10^{-4} M	0.54	0.23	0.46	3.9
4.75×10^{-4} M	0.71	0.13	0.29	3.5
1 mM	0.82	0.094	0.18	2.6
2 mM	0.90	0.094	0.10	2.0
2.9 mM	0.94	0.094	0.06	1.7

3. The KIE value is 2.4, which is similar to the value found in previous studies for D-luciferin and oxyluciferin.
4. In water–methanol mixtures, the ESPT rate decreases as the methanol content becomes higher. L cannot undergo ESPT in neat methanol.
5. Even in the presence of low excess proton concentration in the solution (milimolar), the steady-state fluorescence intensities of both the protonated and deprotonated forms are strongly suppressed. The time-resolved emission exhibits a large drop in the average decay time as well.

DISCUSSION AND DATA ANALYSIS

The results shown in Figures 1–5 clearly indicate that L, like the other two luciferin molecules that we previously studied, D-luciferin and oxyluciferin, is a photoacid. Photoacids are weak acids in the electronic ground state with pK_a's ranging from 9 to 4 and much stronger acids in the lowest excited electronic singlet state. Usually, the difference in the pK_a between the ground and excited states is higher than seven logarithmic units. The radiative lifetimes of the allowed transitions are about 10 ns or shorter. ESPT to the solvent occurs within this time window, and therefore, the ESPT rate coefficient is larger than 10^8 s^{-1}. After ESPT to water occurs, the solvated proton, the hydronium ion, may geminately recombine with the conjugate base of the photoacid to re-form the protonated form with the assistance of diffusion motion. For the luciferins, shown in Scheme 2, the nitrogen in the benzothiazole ring complicates the simple diffusion-assisted recombination process. The heteroatomic nitrogen is a stronger base in the excited state. It is also known that the recombination of the proton with the nitrogen leads to fluorescence quenching. In previous publications on the photophysics and photochemistry of the luciferins, we adopted an extended scheme that illustrates the elementary processes that the luciferins undergo upon photoexcitation (see Scheme 3).[11–16]

Upon photoexcitation of the ground-state neutral protonated form, designated as NROH in the scheme, ESPT to the solvent takes place and produces NRO^-* and a solvated proton. The proton geminate recombination (reverse reaction) leads to ground-state NROH (k_q^{H+} in Scheme 3). About half of the excited-state proton-transfer events end by fluorescence quenching, whereas in the other events, the proton is further

dx.doi.org/10.1021/jp308818r | J. Phys. Chem. A 2012, 116, 10770–10779

removed from the NRO^{-}* molecules by a proton diffusion to the bulk. The geminate proton can recombine with NRO^{-}* at longer times by diffusion-assisted reaction that can be mathematically formulated by the Debye−Smoluchowski equation (designated as the DSE arrow in the scheme). The complexity of this reaction lies in the effective geminate recombination with the proton that leads to fluorescence quenching of the deprotonated form, NRO^{-}. There are two nitrogen atoms in the heterocyclic backbone of the luciferins that can function as potential photobases. Upon excitation, these nitrogens may increase their basicity, so that they may snatch a proton from a nearby water molecule or react with a diffusing proton that was transferred to the solvent and form $^{+}HNRO^{-}$.

Water−Methanol Mixtures. In the previous section, we described the experimental results of L in water−methanol mixtures. In this section, we translate the fluorescence data to plots of ESPT rate coefficient versus the water−methanol mixtures' composition. The fluorescence decay of the protonated form increases the higher the water content in the mixture. As mentioned above, the decay curves of the NROH* form are nearly exponential. We obtained the ESPT rate coefficients from the average decay times, τ_{av}, by integrating the signals over time. Table 1 provides the values of τ_{av} obtained from the L signals from the various water−methanol mixtures. The longest decay time of the NROH* species, 2.33 ns, is obtained from the neat methanol solution. We assume that in pure methanol, the ESPT rate is much slower than $k_F \simeq 1/\tau_{av}^{meOH} = 4.15 \times 10^8\ s^{-1}$, where τ_{av}^{meOH} is the emission lifetime of the NROH* form in neat methanol in the absence of an ESPT process. To obtain the values of k_{PT} of L in water−methanol mixtures, we simply subtract the emission rate coefficient, k_F, from the fluorescence decay rate coefficient, $k = 1/\tau$, of the NROH* form in a water−methanol mixture of a given composition

$$k_{PT} = k - k_F \tag{3}$$

Figure 10 shows the plot of log k_{PT} versus the mole fraction of methanol in the mixture. The decrease in the value of k_{PT} with increasing mole fraction is nonlinear. Until an 0.8 mol fraction of methanol, the decrease in k_{PT} is moderate and almost linear. By this point, k_{PT} decreases by only a factor of 5. Upon further increase of the methanol concentration, k_{PT} drops sharply as the slope of the curve becomes steeper. At a water concentration of 0.015, the ESPT rate coefficient has a value of $\sim 10^8\ s^{-1}$. Similar dependence of the ESPT process on the water content of the mixture in water−methanol mixtures was previously found for photoacids with $pK_a^* \geq 0.4$. For stronger photoacids with $pK_a^* \leq 0$, we found that ESPT occurs even in neat methanol, where the k_{PT}^{meOH} value was equal to or higher than $2 \times 10^8\ s^{-1}$.

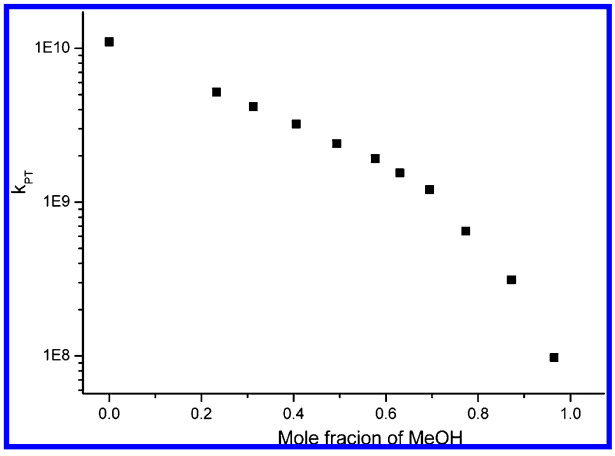

Figure 10. Plot of log k_{PT} versus the mole fraction of methanol in the mixture. Note that the decrease in the value of k_{PT} with increasing mole fraction is nonlinear.

Qualitative Explanation to the Acid Effect on L. In a previous study on D-luciferin,[11−16] the natural substrate of the firefly luciferase, in acidic solution, we found that at a pH level of about 1 (100 mM of HCl), the ground-state D-luciferin undergoes a protonation process. The emission spectrum of D-luciferin in a $c \geq 20$ mM acidic aqueous solution has a new emission band at 590 nm red-shifted with respect to the strongest emission band at 530 nm in a neutral aqueous solution. We attributed the new emission band to the zwitterion form designated as $^{+}HNRO^{-}$. The time-resolved emission signals show that the NRO^{-}* of the D-luciferin emission band at 530 nm and the zwitterion emission band at 590 are strongly quenched by a recombination process with an excess proton in an acidic aqueous solution. The recombination process is nearly diffusion-controlled, where $D_{H^+} = 0.9 \times 10^{-4}$ cm^2/s. The diffusion-controlled rate coefficient is given by

$$k_D \cong 4\pi N' D_{H^+} R_D \tag{4a}$$

where $N' = N_A/1000$ and N_A is Avogadro's number. R_D is the Debye radius, which is given by the following expression:

$$R_D = \frac{ze^2}{4\pi\varepsilon_0 \varepsilon k_B T} \tag{4b}$$

where z is the ionic charge of the NRO^{-}* form, e is the electronic charge, ε_0 is the permittivity, ε is the dielectric constant of the solvent (for water, $\varepsilon = 78$), and k_BT is the thermal energy. The R_D value of luciferins is ~7 Å; hence, $k_{D_{H+}} \simeq 5 \times 10^{10}\ M^{-1}\ s^{-1}$. In acidic samples, the second-order diffusion-controlled recombination rate coefficient is $k_{D_{H+}}$, and the actual proton quenching rate of the NRO^{-}* fluorescence linearly depends on the product of this coefficient with the acid concentration. Figure S5 in the SI shows the time-resolved emission of the NRO^{-}* form of D-luciferin in aqueous solutions of 2, 3, and 4 mM HCl. The fluorescence decay time of the long-time component decreases as the acid concentration increases, whereas the short-time decay component is unaffected by this change. As opposed to the relatively mild acid effect on D-luciferin, the acid effect on the short-time component of L is much more pronounced, and it is already noticeable even at the low concentration of ~0.2 mM. Figure S6a in the SI shows the acid effect on the steady-state emission spectrum of D-luciferin. As seen in the figure, the fluorescence intensity of the NRO^{-}* band decreases as the acid concentration increases. While the fluorescence intensity of the NRO^{-}* band of D-luciferin decreases by a factor of 2, that of L decreases by a factor of 10 even at the low concentration of 2 mM. Addition of 2 mM HCl only affects the lifetime of the long-time component of the NRO^{-}* of D-luciferin. L, however, experiences the acid effect to a much greater extent as it impacts both the lifetime and amplitude of the short-time component, as can be seen in Figure 8b. At 1 mM, the pseudo-first-order reaction rate coefficient's value is $5 \times 10^7\ s^{-1}$, whereas k_F', the radiative rate coefficient, is 10 times larger, 2×10^8 ($\tau_{NRO^{-}*} = 5.2$ ns). We cannot therefore expect excess

dx.doi.org/10.1021/jp308818r | J. Phys. Chem. A 2012, 116, 10770−10779

protons at concentrations of up to 1 mM to have a significant effect on the fluorescence decays of both the NROH* and NRO^-* forms of L.

This explains what is seen in Figure 9b. The NROH* decay is not affected by the introduction of acid until its concentration reaches 1 mM. At neutral pH, the lifetime is 80 ps, and it drops to about 50 ps in the concentration range of 1−3 mM HCl. The steady-state and time-resolved emission spectra of the NRO^-* species, however, feel the effect of the acid from a concentration 10 times lower, that is, 0.2 mM. The intensity of the steady-state emission spectrum is reduced, and the decay profile of the time-resolved signal already changes from this low acid concentration. The amplitude of the short-time component increases from 0.2 in neutral pH solution to 0.9 in 3 mM HCl. The lifetime of the short-time decay component also decreases as the acid concentration increases. At 3 mM, the value of this lifetime is ∼100 ps, whereas in neutral pH, it is 500 ps. The lifetime of the long-time component of the NRO^-* band begins to be affected by the acid at concentrations higher than 1 mM, and the effect on this lifetime is in accord with what is expected from the diffusion-controlled reaction. We fit the time-resolved emission data from several solutions of varying acid concentrations with biexponential functions. The fitting parameters are given in Tables 2 and 3 for the NROH* and NRO^-* species, respectively.

The surprisingly strong acid effect on the NRO^-* band of L can be explained by the fact that the heterocyclic nitrogen atom in the benzothiazole ring is easily protonated by an excess proton in the ground state even at 2×10^{-4} M. When the $^+$HNROH species is excited, it undergoes ESPT to form the $^+$HNRO$^-$* form, which then undergoes a fast fluorescence quenching with a time constant of ∼100 ps. The change in the amplitude of the short-time component indicates that the protonation reaction of the heterocyclic nitrogen in the ground state depends on the acid concentration, as can be expected from the following chemical equilibrium: ($H^+ + NROH \overset{k_{eq}}{\rightleftarrows} {}^+HNROH$). The $^+$HNROH/NROH ratio increases the higher the acid concentration. Figure 11 shows the fluorescence intensity of the yellow emission band at ∼550 nm of both D-luciferin and L as a function of the acid concentration. The fluorescence intensity of L decreases sharply when the acid concentration approaches 1 mM. We attribute the large drop to the protonation of the nitrogen of the thiazole ring. We estimate that its pK_a is ∼3. This is accord with the findings of Haake et al.,[28] who measured the pK of thiazole and its derivatives. They found that its value is about 3. As mentioned above, we attribute the short-time component of the emission band at 550 nm to the $^+$HNRO$^-$* species, which is the product of the protolytic reaction when the reactant is $^+$HNROH*. At 4.7 mM, the protonation level is about 95%, as can be inferred from the fit to the time-resolved emission at 550 nm. The fluorescence intensity of the NRO^-* band of D-luciferin only mildly decreases with addition of acid and only at concentrations higher than 10 mM (see Figure 11). We are not yet certain as to why the NRO^-* fluorescence of L is much more sensitive to protonation of the nitrogen than D-luciferin and why the pK_a differs by more than one unit.

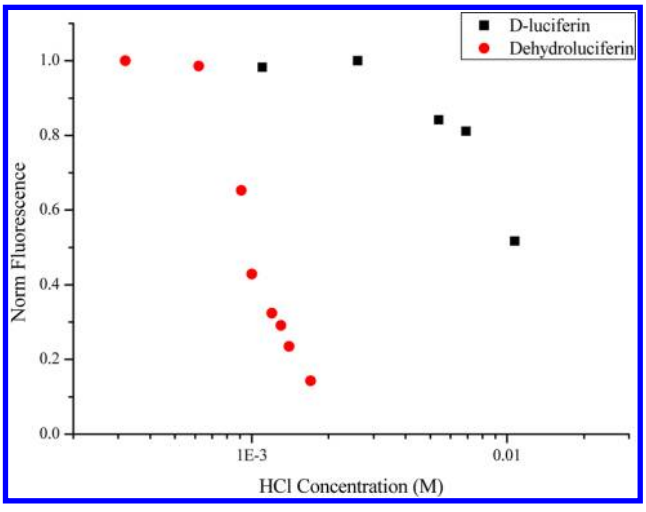

Figure 11. Steady-state spectra of the $^+$HNRO$^-$* emission band of both D-luciferin and dehyroluciferin in various HCl concentrations. Note how the relative fluorescence intensity changes as a function of the acid concentration.

SUMMARY

In the present work, we studied the photophysics and photochemistry of L, a nonbioluminescent chromophore of the firefly.

We found that L is a photoacid with an ESPT rate coefficient of 1.1×10^{10} s^{-1} and τ_{PT} = 88 ps. Previously, we found that D-luciferin and oxyluciferin transfer a proton to water with τ_{PT} values of 27 and 47 ps, respectively. D-Luciferin is a strong enough photoacid so as to transfer a proton to methanol. Only strong photoacids with pK_a* ≤ 0 can transfer a proton to aliphatic monols. After systematic study of the ESPT process of dehydroluciferin in water−methanol mixtures, we expectedly found that its ESPT rate decreases the higher the methanol content in the solution. The plot of the ESPT rate coefficient as a function of the mole ratio of methanol is nonlinear and similar in its shape to those of other photoacids, such as HPTS, 2-naphthol, and 5-cyano-2-naphthol. At a methanol mole ratio of 0.8, the ESPT rate decreases sharply by more than an order of magnitude as the methanol's mole ratio increases to 0.95.

We also conducted a study on the ESPT of L in aqueous solutions containing a strong acid. Surprisingly, a very strong acid effect on both the protonated and deprotonated forms' emissions was found. The steady-state fluorescence of both emission bands decreases as the acid concentration increases (see Figure 8). A significant decrease is noticeable even at concentrations as low as a few millimolars. At these low acid concentrations, the diffusion-controlled irreversible recombination reaction with a proton (NRO^-* + $H^+ \overset{k_D}{\rightarrow}$ NROH(g)) is ineffective because the pseudo-first-order rate coefficient is the product of k_D and the proton concentration, and because $k_D = 5 \times 10^{10}$ M^{-1} s^{-1} and the proton concentration is $\sim 10^{-3}$ M, its value is only $\sim 5 \times 10^7$ s^{-1}, which is four times smaller than the radiative rate coefficient, that is, 1.8×10^8 s^{-1}. The effective fluorescence quenching can be explained by ground-state protonation of the thiazole nitrogen. We found that the pK_a of this reaction for L is ∼3. This is accord with the findings of Haake et al.,[28] who measured the pK of thiazole and its derivatives. They found that its value is about 3. In a neutral aqueous solution, the deprotonated forms of the three luciferin molecules undergo an irreversible geminate recombination (fluorescence quenching by a proton) that is manifested by bimodal fluorescence decay curves at $\lambda \geq 540$ nm (see Scheme 2). The K_b of the nitrogen in the thiazole ring of L is probably

higher than those of the other two luciferins. The fluorescence of the $^{+}HNRO^{-}$* species, that is, the NRO^{-}* form protonated in its nitrogen site, is quenched within 100 ps. This leads us to conclude that the short-time decay component of the time-resolved fluorescence of the long wavelength band can be attributed to both $^{+}HNRO^{-}$* and NRO^{-}* forms. As the acid concentration rises, so does the amplitude of the short-time component, attributed to the $^{+}HNRO^{-}$* form. We also found that the fluorescence decay of the $^{+}HNROH$* species emitting at 450 nm is shorter than 50 ps, that is, shorter than that of the NROH*, whose lifetime is ∼80 ps.

■ ASSOCIATED CONTENT

Supporting Information

Additional figures of dehydroluciferin on a linear scale, D-luciferin in acidic solution, dehydroluciferin in basic solution, and parameter tables of exponential fits to time-resolved data of dehydroluciferin. This material is available free of charge via the Internet at http://pubs.acs.org.

■ AUTHOR INFORMATION

Corresponding Author

*E-mail: huppert@tulip.tau.ac.il. Tel: 972-3-6407012. Fax: 972-3-6407491.

Notes

The authors declare no competing financial interest.

■ ACKNOWLEDGMENTS

This work was supported by grants from the Israel Science Foundation and from the James-Franck German−Israeli Program in Laser-Matter Interaction. Financial support from Fundação para a Ciência e Tecnologia (FCT, Lisbon) (Programa Operacional Temático Factores de Competitividade (COMPETE) e comparticipado pelo Fundo Comunitário Europeu (FEDER) (Project PTDC/QUI/71366/2006) is acknowledged. A Ph.D. grant to Luís Pinto da Silva (SFRH \76612\2011), attributed by FCT, is also acknowledged.

■ REFERENCES

(1) Marques, S. M.; Esteves da Silva, J. C. G. *IUBMB Life* **2009**, *61*, 6−17.
(2) Viviani, V. R.; Arnoldi, F. G.; Neto, A. J.; Oehlmeyer, T. L.; Bechara, E. J.; Ohmiya, Y. *Photochem. Photobiol. Sci.* **2008**, *7*, 159−169.
(3) Pinto da Silva, L.; Esteves da Silva, J. C. G. *ChemPhysChem* **2012**, *13*, 2257−2262.
(4) Pinto da Silva, L.; Esteves da Silva, J. C. G. *J. Chem. Theory Comput.* **2011**, *7*, 809−817.
(5) Pinto da Silva, L.; Esteves da Silva, J. C. G. *J. Phys. Chem. B* **2012**, *116*, 2008−2013.
(6) Pinto da Silva, L.; Esteves da Silva, J. C. G. *ChemPhysChem* **2011**, *12*, 3002−3008.
(7) Pinto da Silva, L.; Esteves da Silva, J. C. G. *ChemPhysChem* **2011**, *12*, 951−960.
(8) Esteves da Silva, J. C. G.; Magalhães, J. M. C. S.; Fontes, R. *Tetrahedron Lett.* **2001**, *42*, 8173−8176.
(9) Song, C.; Rhee, Y. M. *J. Am. Chem. Soc.* **2011**, *133*, 12040−12049.
(10) Naumov, P.; Ozawa, Y.; Ohkubo, K.; Fukuzumi, S. *J. Am. Chem. Soc.* **2009**, *131*, 11590−11605.
(11) Erez, Y.; Presiado, I.; Gepshtein, R.; Pinto da Silva, L.; Esteves da Silva, J. C. G.; Huppert, D. *J. Phys. Chem. A* **2012**, *116*, 7452−7461.
(12) Erez, Y.; Huppert, D. *J. Phys. Chem. A* **2010**, *114*, 8075−8082.
(13) Presiado, I.; Erez, Y.; Huppert, D. *J. Phys. Chem. A* **2010**, *114*, 9471−9479.
(14) Presiado, I.; Erez, Y.; Huppert, D. *J. Phys. Chem. A* **2010**, *114*, 13337−13346.
(15) Erez, Y.; Presiado, I.; Gepshtein, R.; Huppert, D. *J. Phys. Chem. A* **2011**, *115*, 1617−1626.
(16) Presiado, I.; Gepshtein, R.; Erez, Y.; Huppert, D. *J. Phys. Chem. A* **2011**, *115*, 7591−7601.
(17) Fontes, R.; Fernandes, D.; Peralta, F.; Fraga, H.; Maio, I.; Esteves da Silva, J. C. G. *FEBS J.* **2008**, *275*, 1500−1509.
(18) Fraga, H.; Fernandes, D.; Fontes, R.; Esteves da Silva, J. C. G. *FEBS J.* **2005**, *272*, 5206−5216.
(19) Ribeiro, C.; Esteves da Silva, J. C. G. *Photochem. Photobiol. Sci.* **2008**, *7*, 1085−1090.
(20) Pinto da Silva, L.; Esteves da Silva, J. C. G. *Photochem. Photobiol. Sci.* **2011**, *10*, 1039−1045.
(21) Fraga, H.; Esteves da Silva, J. C. G.; Fontes, R. *Tetrahedron Lett.* **2004**, *45*, 2117−2120.
(22) Fraga, H.; Esteves da Silva, J. C. G.; Fontes, R. *FEBS Lett.* **2003**, *543*, 37−41.
(23) Bowie, L. *J. Methods Enzymol.* **1978**, *57*, 15−28.
(24) Pines, E.; Huppert, D.; Agmon, N. *J. Chem. Phys.* **1988**, *88*, 5620−5630.
(25) Presiado, I.; Erez, Y.; Gepshtein, R.; Huppert, D. *J. Phys. Chem. C* **2009**, *113*, 20066−20075.
(26) Tolbert, L. M.; Solntsev, K. M. *Acc. Chem. Res.* **2002**, *35*, 19−27.
(27) Agmon, N.; Huppert, D.; Masad, A.; Pines, E. *J. Phys. Chem.* **1991**, *95*, 10407−10413.
(28) Haake, P.; Bausher, L. P. *J. Phys. Chem.* **1968**, *72*, 2213−2217.